This article was downloaded by:
On: *25 January 2011*
Access details: *Access Details: Free Access*
Publisher *Taylor & Francis*
Informa Ltd Registered in England and Wales Registered Number: 1072954 Registered office: Mortimer House, 37-41 Mortimer Street, London W1T 3JH, UK

Separation Science and Technology
Publication details, including instructions for authors and subscription information:
http://www.informaworld.com/smpp/title~content=t713708471

SANS Study of HCl Extraction by Selected Neutral Organophosphorus Compounds in *n*-Octane

R. Chiarizia[a]; D. Stepinski[a]; M. R. Antonio[a]
[a] Chemical Sciences and Engineering Division, Argonne National Laboratory, Argonne, IL, USA

Online publication date: 30 August 2010

To cite this Article Chiarizia, R. , Stepinski, D. and Antonio, M. R.(2010) 'SANS Study of HCl Extraction by Selected Neutral Organophosphorus Compounds in *n*-Octane', Separation Science and Technology, 45: 12, 1668 — 1678
To link to this Article: DOI: 10.1080/01496395.2010.493828
URL: http://dx.doi.org/10.1080/01496395.2010.493828

PLEASE SCROLL DOWN FOR ARTICLE

Full terms and conditions of use: http://www.informaworld.com/terms-and-conditions-of-access.pdf

This article may be used for research, teaching and private study purposes. Any substantial or systematic reproduction, re-distribution, re-selling, loan or sub-licensing, systematic supply or distribution in any form to anyone is expressly forbidden.

The publisher does not give any warranty express or implied or make any representation that the contents will be complete or accurate or up to date. The accuracy of any instructions, formulae and drug doses should be independently verified with primary sources. The publisher shall not be liable for any loss, actions, claims, proceedings, demand or costs or damages whatsoever or howsoever caused arising directly or indirectly in connection with or arising out of the use of this material.

Separation Science and Technology, 45: 1668–1678, 2010
Copyright © Taylor & Francis Group, LLC
ISSN: 0149-6395 print/1520-5754 online
DOI: 10.1080/01496395.2010.493828

Taylor & Francis
Taylor & Francis Group

SANS Study of HCl Extraction by Selected Neutral Organophosphorus Compounds in *n*-Octane

R. Chiarizia, D. Stepinski, and M. R. Antonio
Chemical Sciences and Engineering Division, Argonne National Laboratory, Argonne, IL, USA

The extraction of HCl by tri(2-ethylhexyl) phosphate (TEHP), tri-*n*-octyl phosphate (TOP), and tri-*n*-octylphosphine oxide (TOPO) in *n*-octane was investigated by liquid-liquid distribution of acid and water and small-angle neutron scattering (SANS) measurements. No formation of a heavy organic phase (third phase) was observed with TEHP and TOP under the experimental conditions used, whereas for 0.4 M TOPO the HCl limiting organic concentration (LOC) at 23°C was 0.32 M (with 5.1 M HCl in the equilibrium aqueous phase). For higher HCl concentrations in the aqueous phase, the organic phase splits into a light and a heavy layer.

For TEHP and TOP, the SANS results, interpreted using the Baxter model for hard spheres with surface adhesion, indicated the formation of only small reverse micelles with little intermicellar attraction. For TOPO, the scattering signals suggested the formation of much larger and strongly interacting micelles. The critical values of the stickiness parameter, τ^{-1}, and the interaction potential energy, $U(r)$, for the LOC sample in the TOPO system were consistent with the model for third-phase formation previously developed for tri-*n*-butyl phosphate (TBP). According to this model, organic phase splitting is due to van der Waals interactions between the polar cores of reverse micelles formed by the extractants in the organic phase.

Keywords Baxter model; distribution isotherm; liquid-liquid extraction; reverse micelle; small-angle neutron scattering; third-phase formation

Downloaded At: 08:40 25 January 2011

INTRODUCTION

Contemporary work has led to a physico-chemical understanding of third-phase formation, the phenomenon by which the organic phase of a solvent extraction system splits into two liquid phases of different compositions and densities (1–16). The authors of these studies have investigated the behavior of extractants of interest for nuclear reprocessing, such as alkyl-substituted malonamides (2,3) and tri-*n*-butyl phosphate (TBP) (4–14) dissolved in *n*-alkane diluents, whereas the aqueous phase generally contained high concentrations of nitric acid and/or metal nitrates.

Received 16 October 2009; accepted 2 April 2010.
Address correspondence to R. Chiarizia, Chemical Sciences and Engineering (CSE) Division, Argonne National Laboratory, Argonne, IL 60439, USA. Fax: 630-252-7501. E-mail: chiarizia@anl.gov

The physico-chemical model developed in these works is based upon the knowledge that the complexes formed by the extractants and the extracted solutes in the organic phase undergo self-assembly, leading to the formation of supramolecular aggregates of the reverse micelle type. The morphology of these aggregates has been investigated through small-angle X-ray and/or neutron scattering (SAXS and SANS, respectively) (2–14). Water, nitric acid, and metal nitrates are incorporated into the polar core of the micelles which interact through van der Waals forces between their polar cores. The separation of most of the solute particles into a new phase takes place when the energy of attraction between the particles in solution becomes significantly larger than the average thermal energy given by k_BT (where k_B = Boltzmann constant). Upon phase splitting, most of the solutes in the original organic phase (extractant, water, nitric acid, and metal nitrates) form a separate and denser third phase that contains only small amounts of diluent.

Studies in which cations such as H^+, UO_2^{+2}, Zr^{+4}, and Th^{+4} (coupled to the same anion, NO_3^-) (4–9,11) were extracted by 20% v/v (0.73 M) TBP in *n*-octane, indicated that the critical energy of interparticle attraction for organic phase splitting was reached more readily for cations possessing a higher charge and a smaller size, for which a more polar micellar core was expected. It was shown that the tendency toward phase splitting correlates well with the hydration enthalpy of the cations (11).

In other studies, third phase formation was investigated for the extraction of HCl (13,14), HNO_3, $HClO_4$, H_2SO_4, and H_3PO_4 (15,16) by TBP in *n*-octane. The series for the tendency to third-phase formation ($HClO_4 > H_2SO_4 > HCl > H_3PO_4 > HNO_3$) correlates with the amount of water present in the organic phase at the critical point of phase splitting (15,16). That result reinforced the validity of the micellar model developed for the extraction of polar solutes by TBP. Upon extraction of inorganic mineral acids, the concomitant presence of large amounts of water in the polar core of the reverse micelles makes the micellar core more polar and, therefore, it increases the strength of the intermicellar attraction, thus facilitating third-phase formation.

Downloaded At: 08:40 25 January 2011

In our quest to identify general trends and unifying mechanisms and energetics for third-phase formation in solvent extraction, we have extended our investigations to third-phase formation with selected neutral organophosphorus extractants characterized by longer alkyl chains and a more polar donor group than TBP (structures in Fig. 1). Extraction of HCl was used as the probe for phase splitting.

For the tri(2-ethylhexyl) phosphate (TEHP) and the tri-*n*-octyl phosphate (TOP) extractants, both with the same polar group as TBP, the C_8 alkyl chains (branched in the case of TEHP) should increase substantially the distance between the polar cores of interacting reverse micelles as compared to TBP whose alkyl chains have only four carbon atoms. Consequently, the expected weaker intermicellar attraction should make third-phase formation more difficult than with TBP under the same conditions.

Although tri-*n*-octylphosphine oxide (TOPO) has the same C_8 alkyl chains as TOP, the P=O donor group for the phosphine oxide is more polar than for the phosphate. For the same distance between the polar cores of interacting micelles, which is determined by the length of the alkyl chains, the more polar cores of the TOPO micelles should generate a stronger intermicellar attraction, which, in turn, should lead to an enhanced tendency to form third phases in TOPO solvent extraction systems as compared to those based on TOP or even TBP.

In this work, we investigated the extraction of HCl by TEHP, TOP, and TOPO and performed SANS measurements on *n*-octane solutions of the extractants at different solute loading levels up to and, when possible, beyond the critical point of phase splitting. The objectives of this work were:

- To measure the distribution isotherms of HCl between water and *n*-octane solutions of TEHP, TOP and TOPO, identifying the critical point of third phase formation (when phase splitting occurs);
- To measure the morphology and composition of the micellar aggregates in the organic phase and how the intermicellar attraction energy evolves as a function of organic phase loading;
- To confirm the general application of the micellar model for third phase formation.

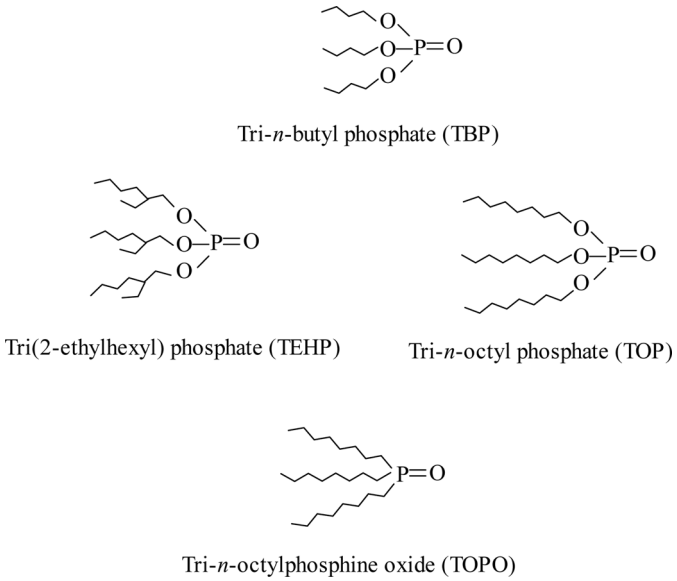

FIG. 1. Structure of TBP and extractants used in this work.

EXPERIMENTAL

Materials

n-Octane and deuterated *n*-octane (d_{18}, 98 atom% D, indicated hereafter as D-octane) were obtained from Aldrich Chemicals. ULTREX® ultra high purity HCl was obtained from J. T. Baker Chemical Co.

Tri(2-ethylhexyl) phosphate (liquid, MW = 434.64) and tri-*n*-octylphosphine oxide (solid, MW = 386.65) were commercial products, obtained from Alfa Aesar and Aldrich Chemicals, respectively. Their purity (>99%) was checked by ^{1}H and ^{31}P NMR.

Tri-*n*-octyl phosphate (liquid, MW = 434.64), a compound not commercially available, was synthesized using the following procedure: a solution of *n*-octyl alcohol (33.8 mL, 0.215 mol) and pyridine (19.1 mL, 0.236 mol) in 50 mL toluene was added dropwise over a 2 hr period to phosphorus oxychloride (5.0 mL, 0.0546 mol) dissolved in 150 mL toluene. After stirring overnight at room temperature under a nitrogen atmosphere, the organic phase was washed with three 50 mL portions of 0.2 M HCl. Toluene and unreacted alcohol were removed from the product mixture by vacuum distillation. The product mixture was then dissolved in methanol and most of the acidic impurities were removed from the methanol solution using the Bio-Rad AG 1-X4, 50–100 mesh, chloride form resin, as described previously (17). Residual acidic impurities were removed using gel flash chromatography (15:85 v/v EtOAc/hexane; $R_f = 0.8$). Finally, the TOP extractant was obtained by removing the solvent under reduced pressure at 60°C. All reagents used in this procedure were supplied by Sigma-Aldrich and used as received. Anhydrous toluene was dispensed from an Aldrich Sure-Seal bottle. The purity of the compound was established by ^{1}H and ^{31}P NMR and by C and H elemental analysis (Galbraith Laboratories, Knoxville, TN): C, 66.32% theoretical, 66.72% found; H: 11.83% theoretical, 12.07 found.

Procedures and Analyses

The procedures used for the solvent extraction experiments and the analytical methods were the same as those

used in our previous studies. Details can be found elsewhere (13–15).

The TOPO concentrations in the heavy and light organic phases resulting from phase splitting were determined, after appropriate sample dilution with *n*-octane and stripping of the acid, from the distribution ratio (D_{Am}) of ^{241}Am (from ANL stocks) between the organic phase samples and 2.3 M HNO_3 by using a calibration curve of D_{Am} vs. TOPO concentration ($\log D_{Am} = (0.73 \pm 0.07) + (2.28 \pm 0.05)\log[\text{TOPO}]$).

Samples for SANS Measurements

The same procedure, as the one used for the solvent extraction experiments, was used, except that D-octane was used as the diluent. The composition of the samples for SANS measurements is summarized in Table 1.

The values of the volume fraction of polar solutes in Table 1 were given by the sum of the volume fractions of HCl, water, and the polar head of the extractants. The polar solutes (HCl plus H_2O) and the polar portion of the extractant molecules (PO_4 or P=O) are located in the polar core of the reverse micelles, whereas the alkyl groups form the hydrophobic shell of the micelles. The molar volumes of H_2O and HCl (13) were taken equal to 18.02 and 18.51 mL, respectively. The molar volumes of the polar and nonpolar portions of the extractant molecules were calculated from the total molar volume (given by the ratio of molecular weight and density) and the Tanford equation for the volume V(Å) of a fully extended hydrocarbon chain with n_c carbon atoms (18): $V = 27.4 + 26.9\ n_c$. For example, for TOP (MW = 434.64 and d = 0.913 g/mL), the total molar volume is 475.95 mL; the nonpolar molar volume is $3(27.4 + 26.9 \times 8)N_{Av}/10^{24} = 438.29$ mL (N_{Av} is Avogadro's number); the polar molar volume is given by the difference: 37.66 mL. For TEHP (MW = 434.64 and

TABLE 1
Composition of samples for SANS measurements (T = 23 ± 0.5°C)

Sample	[Extractant][a] M	[HCl][a] M	[H_2O][a] M	Polar solutes volume fraction	Total solutes volume fraction
TEHP					
10	0.403	0	0.0429	0.0159(3)	0.189(4)
11	0.403	0.0299	0.0744	0.0171(3)	0.190(4)
12	0.403	0.0570	0.0871	0.0178(3)	0.191(4)
13	0.403	0.265	0.147	0.0227(4)	0.196(4)
TOP					
20	0.403	0	0.0414	0.0159(3)	0.193(4)
21	0.403	0.0457	0.119	0.0182(4)	0.195(4)
22	0.403	0.0811	0.154	0.0195(4)	0.196(4)
23	0.403	0.273	0.227	0.0243(5)	0.201(4)
30	0.686	0	0.216	0.0297(6)	0.330(7)
31	0.686	0.123	0.339	0.0342(8)	0.335(7)
32	0.686	0.180	0.424	0.0368(9)	0.338(7)
33	0.686	0.588	0.883	0.0526(17)	0.353(7)
TOPO					
40	0.300	0	0.0336	0.0051(1)	0.137(3)
41	0.403	0.183	0.531	0.0190(9)	0.196(4)
42	0.403	0.262	0.518	0.0203(9)	0.107(4)
43	0.403	0.298	0.504	0.0207(9)	0.197(4)
44 (LOC)[b]	0.403	0.321	0.480	0.0207(5)	0.197(4)
45 (Heavy Phase)[c]	1.03	1.47	0.875	0.0585(1)	0.51(2)
46 (Light Phase)[c]	0.006	0.0079	0.0332	0.00084(8)	0.0035(1)

Notes. [a]Estimated accuracies are ±2% for the extractant (±5% for light and third phases), ±2% for the acid, and ±10% for water concentration respectively.

[b]LOC stands for Limiting Organic Concentration, i.e., the highest organic phase HCl concentration that can be reached without phase splitting.

[c]Initial conditions: 4.0 mL 0.403 M TOPO in D-octane equilibrated with 4.0 mL 10.0 M HCl. After centrifugation, the original organic phase was distributed between 1.6 mL heavy organic phase (third phase, sample 45) and 2.4 mL light organic phase (sample 46).

Downloaded At: 08:40 25 January 2011

d = 0.930 g/mL), similarly, the total molar volume is 467.36 mL, the polar molar volume must be the same as for TOP (37.66 mL), and the nonpolar molar volume can be obtained by difference: 429.70 mL. In the case of TOPO (MW = 386.65 and unknown density), the nonpolar molar volume must be the same as for TOP (438.29 mL), the polar molar volume can be taken as 2/5 of the value for TOP (15.06 mL) and, therefore, the total molar volume is 453.36 mL, which corresponds to a density of 0.853 g/mL.

SANS Measurements

The SANS measurements were performed at the time-of-flight small-angle neutron diffractometer (SAND) at the Intense Pulsed Neutron Source of Argonne National Laboratory (19) before the IPNS facility was shut down in 2008. The main characteristics of the SAND diffractometer have been described previously (6,7). The samples were measured in standard Suprasil cells with a pathlength of 2 mm and a sample volume of 0.8 mL. The data collection time was three hours per sample. For each sample the data were collected as scattered intensity, $I(Q)$ (cm^{-1}), vs. momentum transfer ($Q = (4\pi/\lambda)\sin(\theta)$ ($Å^{-1}$)), where θ is half the scattering angle and λ is the wavelength of the probing neutrons. The contrast between the solutes and the solvent is mostly determined by the different neutron scattering properties of the H atoms of the extractants and the D atoms of D-octane. For each sample the contrast factor was calculated from the scattering length densities of the D-octane diluent and the various solutes by using the sample compositions in Table 1.

Calculations

To derive quantitative information on the structure and interaction of reverse micelles from the SANS data, we used the following equation describing scattering by a monodisperse system of particles:

$$I(Q) = N_p V_p^2 (\rho_p - \rho_s)^2 P(Q) S(Q) + I_{inc} \qquad (1)$$

where $I(Q)$ is the intensity of the neutrons scattered by the micelles (obtained from the experimental scattering intensities by subtracting the intensities measured for the diluent alone multiplied by the diluent volume fraction in the sample), N_p is the number of micelles per unit volume, V_p is the volume of micelles, $(\rho_p - \rho_s)^2$ is the contrast factor (the difference in the scattering length densities of the micelles and diluent), $P(Q)$ is the single particle form factor, which describes the size and shape, $S(Q)$ is the structure factor, which accounts for the interaction between the scattering particles, and I_{inc} is the incoherent scattering background (20).

For the best fits to the SANS data, we assumed the scattering particles to be spherical. In this case, the form factor, $P(Q)$, in Eq. (1) can be written as:

$$P(Q) = \frac{3[\sin(QR) - QR\cos(QR)]^2}{(QR)^3} \qquad (2)$$

where R is the radius of the sphere (20).

The evaluation of the extent of interaction between particles was performed using the Baxter model for hard spheres with surface adhesion, following the procedure described previously (13,14,16,21). According to this model, the approximate value of the potential energy of attraction (which is negative) between two hard spheres, $U(r)$, expressed in k_BT units, is given by the following equation:

$$U(r) = \lim_{\delta \to d_{hs}} \ln\left[12\tau\left(\frac{\delta - d_{hs}}{d_{hs}}\right)\right] \qquad (3)$$

where d_{hs} is the diameter of the hard spheres and $(\delta - d_{hs})$ represents the width of a narrow square attractive well. When the distance between two particles is larger than d_{hs} but smaller than δ (i.e., for $d_{hs} < r < \delta$), the particles experience attraction. Use of Eq. (3) requires knowledge of the parameter τ. This parameter is the reciprocal of the "stickiness parameter," τ^{-1}, and its value increases directly with the strength of the attraction between particles. The Baxter model provides analytical expressions for the structure factor, $S(Q)$, in Eq. (1) (22,23).

RESULTS AND DISCUSSION

Extraction of HCl by TEHP and TOP

Figure 2 shows the HCl distribution isotherms for 20% (v/v) (0.403 M) TEHP and TOP in *n*-octane. Data are also included for 33% (v/v) (0.686 M) TOP, a molar concentration comparable to that used in our study of HCl extraction by TBP (13). The data indicate that no organic phase splitting occurs with these two extractants even when they are equilibrated with concentrated HCl (~12 M). The effect of branching of the alkyl groups of the extractant is almost negligible except for a small increase of acid extraction with TOP as compared with TEHP at the same concentrations.

By recalling that with 20% (v/v) TBP (0.73 M) in *n*-octane a third phase appears for initial aqueous concentrations of HCl higher than 7.6 M (13), the data in Fig. 2 support our micellar model for third phase formation: the C_8 alkyl chains (branched in the case of TEHP), increase substantially the distance between the polar cores of interacting reverse micelles as compared to the case of TBP. This increased separation makes the intermicellar attraction weak and, therefore, third-phase formation is impossible under the conditions of this work.

Downloaded At: 08:40 25 January 2011

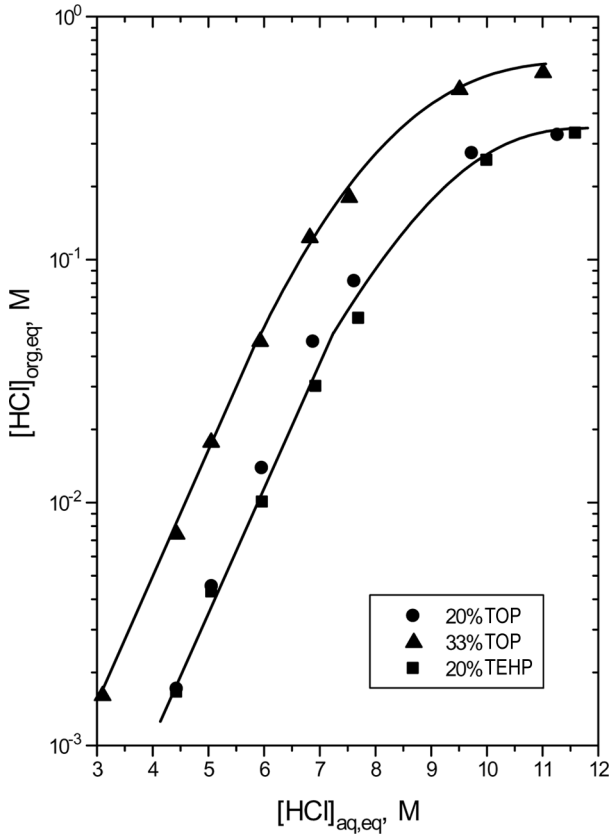

FIG. 2. Isotherms for the extraction of HCl by 20% (v/v) (0.403 M) TOP, 33% (v/v) (0.686 M) TOP, and 20% (v/v) (0.403 M) TEHP in *n*-octane at 23 ± 0.5°C. The lines are a guide for the eye.

Extraction of HCl by TOPO

Figure 3 shows the simplified phase diagrams for the distribution of HCl, TOPO and H_2O (left, center, and right panels, respectively) between 0.403 M TOPO in *n*-octane and HCl aqueous solutions at 23 ± 0.5°C. For this system, the data show that third-phase formation is observed at an HCl aqueous equilibrium concentration of 5.08 M which corresponds to an initial concentration of 5.31 M.

This HCl concentration is significantly lower than that required for phase splitting when the extractant is TBP, i.e., 7.6 M (13). In a TOPO solvent extraction system, compared to TBP, the longer alkyl chains reduce the tendency to third phase formation (*vide supra*). However, the increased basicity of the P=O donor group makes the cores of the TOPO micelles more polar leading to enhanced tendency to form third phases. The latter effect predominates and makes third phase formation occur at a lower aqueous HCl concentration for TOPO than for TBP. The effect of the donor group basicity is obviously also the reason why phase splitting takes place in the extraction of HCl by TOPO whereas it does not with TOP that has the same alkyl groups.

In the simplified phase diagrams of Fig. 3 (left), the critical point corresponding to the HCl limiting organic concentration (LOC = 0.321 M) is identified by the intersection of the three curves describing the organic phase HCl concentrations in the biphasic and triphasic regions of the diagram. When a 0.403 M TOPO solution in *n*-octane is equilibrated with an aqueous phase having an HCl concentration higher than that corresponding to

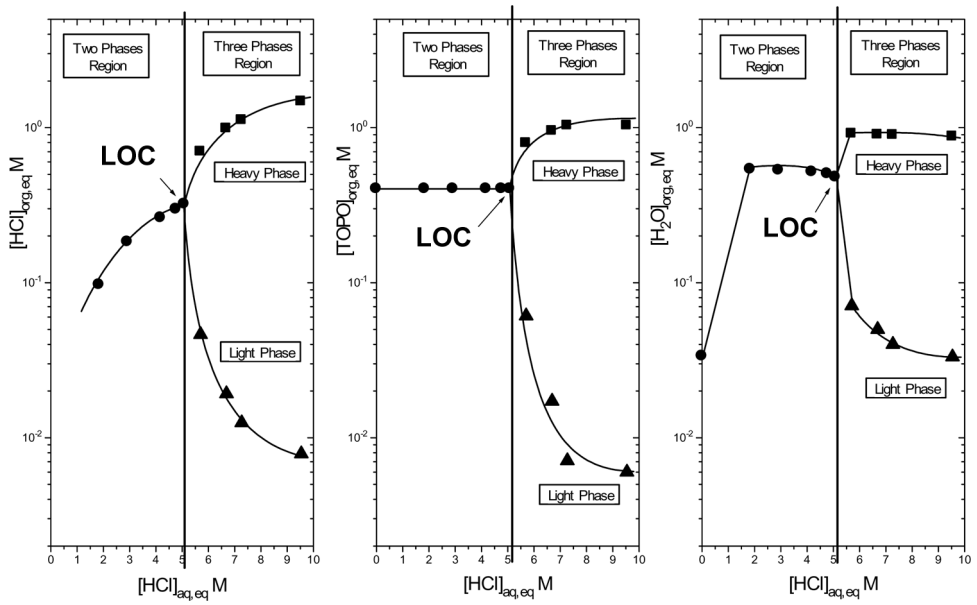

FIG. 3. Simplified phase diagrams for the distribution of HCl (left panel), TOPO (center panel) and H_2O (right panel) between *n*-octane and HCl aqueous solutions at 23 ± 0.5°C. The lines are a guide for the eye.

Downloaded At: 08:40 25 January 2011

the LOC condition, the organic phase splits into two layers. The HCl concentrations in the two organic phases resulting from third phase formation are described by the curves in the triphasic regions of Fig. 3 (left).

As it appears in Fig. 3, all the solutes in the organic phase (HCl, TOPO, and H_2O) distribute asymmetrically between the light and heavy organic phases, reporting mostly in the heavy layer, whereas the light organic phase is a very dilute solution of the various solutes. The values of the [TOPO]:[HCl] ratios in the four third phases of Fig. 3 vary between 1.1 and 0.7, indicating that the average composition of the predominant species in each of the third phases is close to that of a monosolvate. Similarly, the values of the [H_2O]:[HCl] ratios (between 1.3 and 0.6) point to a variable degree of hydration of the HCl · TOPO monosolvate, including a monohydrate and a hemihydrate species.

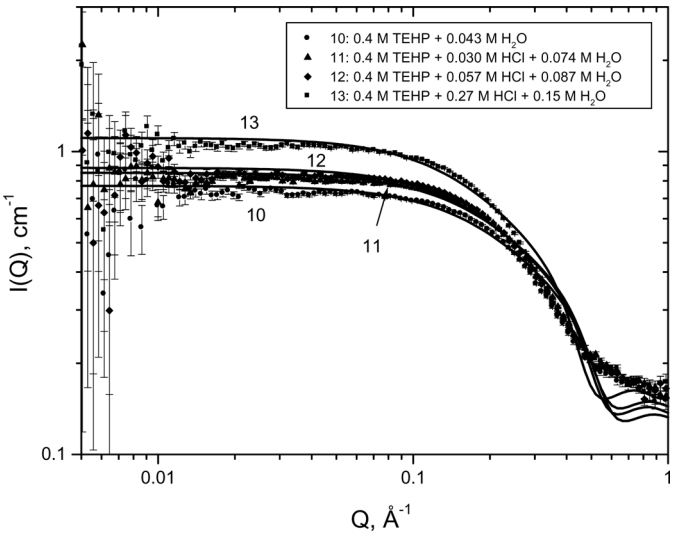

FIG. 4. SANS data and Baxter model fit for HCl-TEHP samples 10, 11, 12, and 13 in Table 1.

SANS Results

To quantitatively evaluate the interaction between particles, the Baxter model was applied to the SANS data for the samples in Table 1 by using Eq. (1) in the form:

$$I(Q) = \eta V_p(\rho_p - \rho_s)^2 P(Q)S(Q) + I_{inc} \qquad (4)$$

which was obtained by introducing into Eq. (1) the solute volume fraction, η, given by the product N_pV_p. Equation (4) was used in conjunction with Eq. (2) for the form factor of a sphere and the analytical expressions for the structure factor, $S(Q)$ (22,23). The three parameters I_{inc}, d_{hs}, and τ were used as fit parameters and were optimized using the procedure described previously (11,13,14,16) and the nonlinear curve fitting features of the Origin™ program (Microcal™ Software, Inc.). The fit was weighted by the experimental statistics of the SANS data. The Origin™ program provided the uncertainty associated with the fit parameters. For simplicity, the particles were assumed to be monodisperse spheres of diameter d_{hs}, which greatly facilitates the fitting procedure.

The Baxter model fits for the TEHP, TOP (0.403 M) and TOPO samples (up to the LOC condition) in Table 1 are shown in Figs. 4–6. Table 2 summarizes the values of the diameter of the hard sphere, d_{hs}, provided by the fits, as well as the other results from the Baxter model calculations that will be discussed below.

For the TOPO third phase (sample 45), the same approach as for third phases in other extraction systems was used (2,8,9,11,13,14,16). Figure 7 shows the fit for the third phase along with that for the corresponding light phase (sample 46).

The fits shown in Figs. 4–7 share a common feature, i.e., a sinusoidal behavior of the calculated $I(Q)$ curves in the high Q range. This behavior is due to the use of Eq. (2) in the Baxter model calculations and to our simplifying assumption of monodisperse particles. Given the inherently soft and flexible nature of reverse micelles, some level of polydispersity is likely, as shown in prior studies of TBP (16) and malonamide extractants (24). To assess its importance in the systems investigated in this study, we introduced polydispersity into the calculations for sample 44 in Table 1 (the LOC sample of the HCl-TOPO system). Figure 8 shows the fit of the data assuming the following symmetrical distribution of sizes: 20%, 60%, and 20% for d_{hs} equal to 18 Å, 26 Å, and 34 Å, respectively. In this distribution of particle sizes, the number average (MW_n)

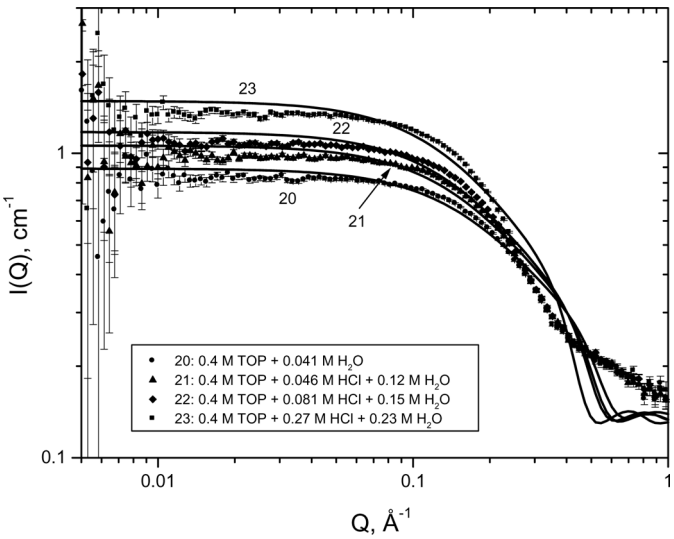

FIG. 5. SANS data and Baxter model fit for HCl-TOP samples 20, 21, 22, and 23 in Table 1.

Downloaded At: 08:40 25 January 2011

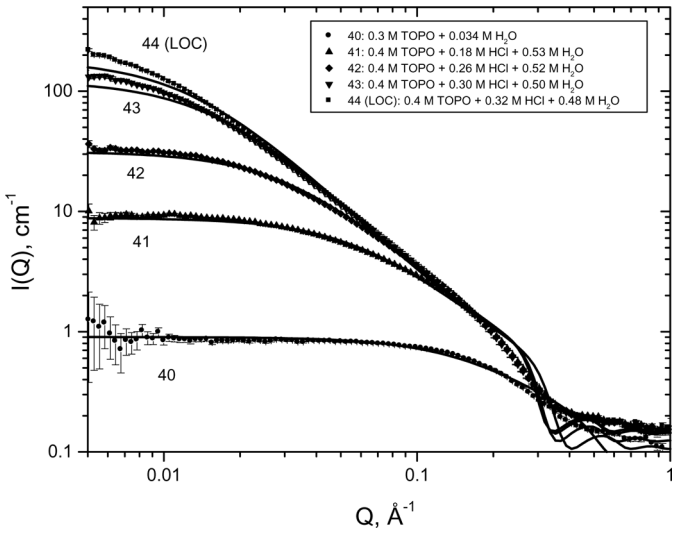

FIG. 6. SANS data and Baxter model fit for HCl-TOPO samples 40, 41, 42, 43, and 44 (LOC) in Table 1.

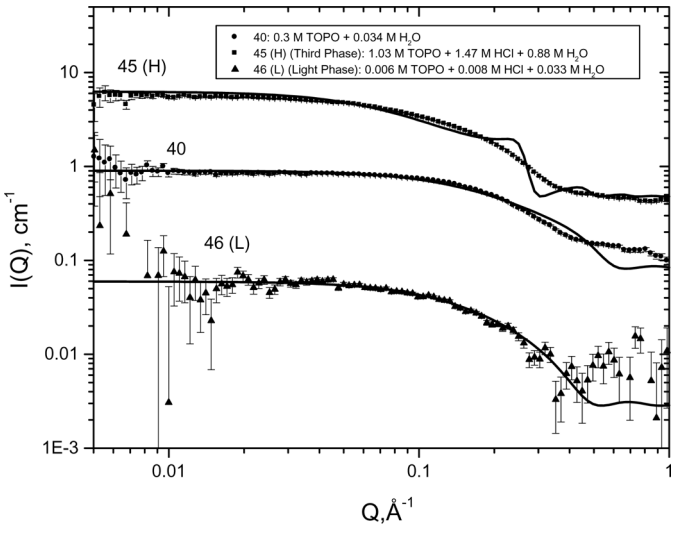

FIG. 7. SANS data and Baxter model fit for HCl-TOPO samples 40, 45 (heavy phase) and 46 (light phase) in Table 1.

Downloaded At: 08:40 25 January 2011

TABLE 2
Results from Baxter model calculations

Sample	d_{hs} [a] Å	d_p [b] Å	Shell[c] Å	n_w [d]	$1/\tau$ [e]	$U(r)$ [f] k_BT
TEHP						
10	13.3(2)	5.8(1)	3.7(1)	1.6(1)	3.6(1)	−1.09(3)
11	13.9(2)	6.2(1)	3.8(1)	1.8(1)	3.5(1)	−1.08(2)
12	14.1(2)	6.4(1)	3.9(1)	1.9(1)	3.6(1)	−1.11(2)
13	16.0(2)	7.8(1)	4.0(1)	2.6(1)	3.6(1)	−1.10(2)
TOP						
20	13.0(2)	5.7(1)	3.7(1)	1.4(1)	4.4(1)	−1.29(3)
21	14.0(2)	6.3(1)	3.7(1)	1.8(1)	4.4(1)	−1.31(3)
22	14.5(2)	6.7(1)	3.9(1)	2.0(1)	4.5(1)	−1.32(3)
23	16.7(2)	8.3(1)	4.2(1)	3.0(1)	4.2(1)	−1.26(3)
30	14.7(2)	6.6(1)	4.1(1)	2.0(1)	4.5(1)	−1.32(3)
31	16.4(2)	7.7(1)	4.4(1)	2.9(1)	4.6(2)	−1.34(3)
32	17.2(2)	8.2(1)	4.5(1)	3.2(1)	4.5(2)	−1.33(3)
33	19.0(2)	10.0(1)	4.5(1)	4.2(2)	4.4(2)	−1.31(3)
TOPO						
40	13.4(2)	4.5(1)	4.5(1)	1.7(1)	4.9(1)	−1.41(3)
41	22.0(2)	10.1(1)	5.9(1)	6.9(2)	7.0(1)	−1.76(2)
42	24.9(2)	11.2(1)	6.6(1)	10.0(2)	8.77(5)	−1.99(1)
43	25.7(2)	12.1(1)	6.8(1)	11.0(3)	9.92(3)	−2.11(1)
44 (LOC)	26.0(2)	12.3(1)	6.9(1)	11.4(3)	10.11(2)	−2.13(1)
45 (Third Ph.)	29.2(7)	14.2(1)	7.5(1)	15.8(9)	14(4)	−2.5(3)
46 (Light Ph.)	16.8(2)	10.4(2)	3.2(1)	2.6(1)	/ [g]	/ [g]

Notes. [a]Hard sphere diameter.
[b]Diameter of polar core; [c]thickness of lipophilic shell.
[d]Weight-average aggregation number of extractant.
[e]Stickiness parameter.
[f]Potential energy of intermicellar attraction.
[g]No measurable interaction.

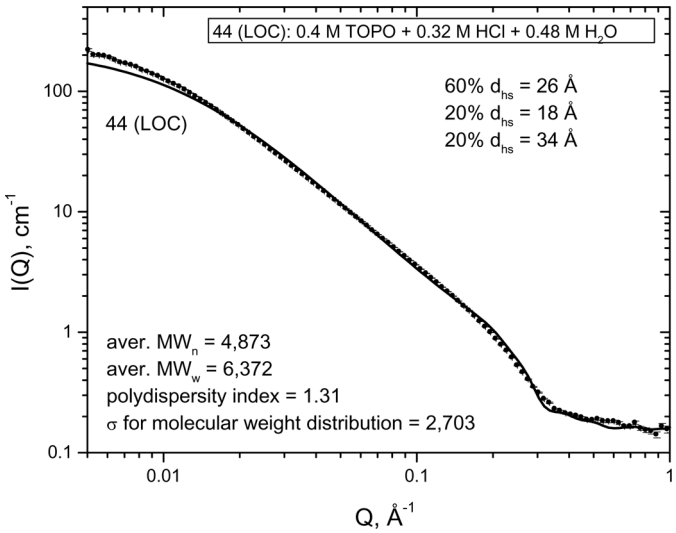

FIG. 8. SANS data and Baxter model fit for HCl-TOPO sample 44 (LOC) in Table 1, with 60% of the reverse micelles having a d_{hs} of 26 Å, 20% a d_{hs} of 18 Å and 20% % a d_{hs} of 34 Å, respectively.

and the weight average (MW_w) molecular weights of the particles are 4,873 and 6,372, respectively, with a polydispersity index (ratio of MW_w to MW_n) of 1.31 and a standard deviation for the molecular weight distribution of 2,703.

Figure 8 shows that the fit of the calculated $I(Q)$ curve to the experimental data is better than without introducing polydispersity (cf. Fig. 6). Notably, the oscillations at high Q values largely disappear. Nonetheless, the use of polydispersity provides values of average d_{hs} and τ that differ only modestly from those calculated with the monodisperse Baxter model. Consequently, the general conclusions about average particle size and the energetics of phase spitting derived from the Baxter model do not change when polydispersity is considered.

The value of the hard sphere diameter obtained for each sample from the Baxter model fit of the SANS data was used to calculate the volume of the scattering particle. This volume comprises both the volume of the polar constituents of the micelle (the polar core) and the volume occupied by the non-polar butyl groups of the extractant (the lipophilic shell). By using the analytical data in Table 1, the volume of the polar micellar core and, hence, its diameter (d_p in Table 2) was calculated by multiplying the total volume of the micelle by the ratio of polar solutes to total solutes volume fraction. The volume of the shell was then estimated by subtracting the volume of the polar core from the total micellar volume, and the shell thickness was obtained from d_{hs} and the diameter of the polar core. Finally, the weight-average aggregation number of the extractant in the micelle, n_w in Table 2, was obtained by dividing the volume of the shell by the nonpolar volume of the extractant.

From the τ values provided by the Baxter fit of the SANS data, the attractive potential energy between two particles, $U(r)$ in k_BT units, was calculated using Eq. (3), by assuming an attractive well width equal to 10% of the hard sphere diameter. The $U(r)$ values are also reported in Table 2 along with the values of the stickiness parameter τ^{-1}.

The average composition of the micelles can be obtained from the values of the extractant aggregation numbers and the sample compositions in Table 1. For example, under the LOC condition, each HCl-TOPO micelle should contain an average of 11.4 molecules of TOPO plus 9.1 molecules of acid and 13.6 molecules of water. The composition of the reverse micelles at the LOC condition for TOPO or at the highest HCl concentration in the organic phase for TEHP and TOP is reported in Table 3, where the number of molecules of the various micellar constituents is approximated to the closest integer value. For comparison, the results obtained earlier for the HCl-TBP system are included in Table 3. Figure 9 shows a schematic representation of the average micelle formed in the HCl-TOPO system.

In spite of the approximations involved in the Baxter model, the results in Table 2 provide a coherent picture of the behavior of the organophosphorus extractants in the extraction of progressively larger amounts of HCl.

When solutions of TEHP (sample 10), TOP (samples 20 and 30), and TOPO (sample 40) in *n*-octane are equilibrated with only water, the extractant aggregation numbers, n_w, are between 1.4 and 2. This behavior is consistent with that of TBP which is known to exist in solution predominantly as simple dimers (25).

For TEHP and TOP, the extraction of large amounts of HCl and water into the organic phase brings about only a modest increase in the size of the micelles, as indicated by the d_{hs} and d_p values in Table 2, and the n_w values remain lower than 3. For 0.686 M TOP, even at the highest concentrations of HCl and H_2O in the organic phase

TABLE 3
Average composition of the reverse micelles for LOC Samples or for highest HCl concentrations in the organic phase

Sample	System	Extractant[a]	Acid[a]	H_2O[a]
13[b]	0.403 M TEHP	3	2	1
23[b]	0.403 M TOP	3	2	2
33[b]	0.686 M TOP	4	4	5
44 (LOC)	0.403 M TOPO	11	9	14
LOC[c]	0.73 M TBP	7	3	3

Notes. [a]Molecules per micelle.
[b]This sample does not represent a LOC condition, as no third phase formation takes place in this system.
[c]From ref. [13].

Downloaded At: 08:40 25 January 2011

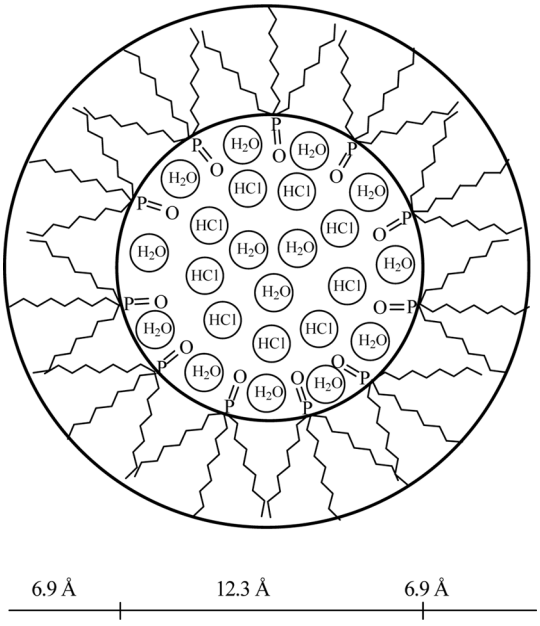

FIG. 9. Schematic representation of the average reverse micelles formed in the HCl-TOPO system at the LOC condition.

Downloaded At: 08:40 25 January 2011

(0.588 and 0.883 M, respectively – see Table 1), the n_w value remains limited to about 4.

The stickiness parameter, τ^{-1}, and the intermicellar attraction energy, $U(r)$, for the TEHP and TOP samples remain far from the values typically obtained for the LOC condition of TBP solvent extraction systems under conditions similar to those of the present work ($\sim$10 and $\sim -2\,k_BT$, respectively) (8,9,11,13,14,16). These results indicate that even high concentrations of HCl and water in the polar core of the micelles (samples 13, 23, and 33) are not sufficient for the intermicellar interactions to become so strong as to produce organic phase splitting. The longer alkyl chains of TEHP and TOP, as compared to TBP, by increasing the distance between the polar cores of the micelles, weaken the intermicellar attraction to the point of making third phase formation impossible under these experimental conditions.

The results in Table 2 present a quite different picture for the HCl-TOPO extraction system. Upon extraction of HCl and water, the TOPO micelles increase considerably in size ($d_{hs} = 26$ Å and d_p 12.3 Å for the 44(LOC) sample), and n_w reaches a value as high as 11. In spite of the long C_8 alkyl chains, these large, swollen micelles (see Fig. 9) interact so strongly through van der Waals forces between their polar cores that the organic phase becomes unstable and splits into two layers. Strong intermicellar attraction is clearly indicated by the values of the stickiness parameter (10.11) and the energy of attraction ($-2.13\,k_BT$), values that are very close to those measured for LOC samples of TBP in the extraction of metal nitrates and inorganic acids (8,9,11,13,14,16). It is interesting to note in this context that the HCl-TOPO-H_2O particles in the third phase (sample 45) are also strongly interacting, as shown by the τ^{-1} and $U(r)$ values in Table 2, whereas no significant interparticle interaction was revealed by the SANS measurements in the very dilute light phase (sample 46).

The thickness of the lipophilic shell of the reverse micelles is the same for TEHP and TOP (about 4 Å) and is therefore insensitive to branching in the alkyl chains of the extractants. The data in Table 2 indicate a thicker shell for the TOPO micelles (6 to 7 Å). This may indicate that without the three hydrophilic phosphate oxygen atoms, the P=O group of TOPO does not penetrate the polar core as deeply as TOP and TEHP. However, for all three extractants the thickness of the lipophilic shell is much smaller than 11.6 Å, the length of a fully extended octyl group calculated through Tanford's equation (18). As previously discussed (16), this result is a clear indication that the alkyl chains of the extractants do not extend perpendicular to the hypothetical surface of the micellar core but wrap around a substantial portion of the polar core.

CONCLUSIONS

In our continuing quest to identify general trends and unifying mechanisms and energetics for third phase formation in solvent extraction, we investigated the extraction of HCl by tri(2-ethylhexyl) phosphate (TEHP), tri-*n*-octyl phosphate (TOP) and tri-*n*-octylphosphine oxide (TOPO) in *n*-octane by liquid-liquid distribution and small-angle neutron scattering (SANS) measurements. TEHP and TOP have the same donor group as TBP, but C_8 alkyl chains (branched in the case of TEHP) instead of C_4 chains. TOPO has the same C_8 alkyl chains as TOP, but a much more polar P=O donor group (phosphine oxide vs. phosphate).

We found that with TEHP and TOP no third phase formation takes place, even when the *n*-octane solution of the extractants is contacted with concentrated HCl. The results of SANS measurements, interpreted by using the Baxter model for hard spheres with surface adhesion, indicated that the reverse micelles formed by TEHP and TOP are always small (aggregation numbers <4) and weakly interacting (very low values of the stickiness parameter and potential energy of attraction).

With TOPO, we observed that the organic phase splits into two layers when contacted with an aqueous phase containing HCl at a concentration higher than 5.31 M. The limiting organic phase concentration of HCl (LOC condition) is 0.321 M. The SANS signals suggested the formation of much larger and strongly interacting micelles. These results are consistent with the model for third phase formation previously developed for TBP. According to this model, organic phase splitting is due to van der Waals

interactions between the polar cores of reverse micelles formed by the extractants in the organic phase. For TEHP and TOP, the increased distance between the polar cores of interacting reverse micelles as compared to TBP makes the intermicellar attraction weaker and third phase formation impossible under the conditions of this work. For TOPO, in spite of the same octyl chains as in TOP, the enhanced basicity of the phosphoryl donor group makes the polar cores of the reverse micelles interact so strongly through van der Waals forces that the organic phase becomes unstable and splits into two layers.

The critical values of the stickiness parameter ($\tau^{-1} = 10.1$) and the interaction potential energy, ($U(r)$, $= -2.13\,k_BT$), for the LOC sample in the TOPO system are the same as those reported previously for third-phase formation in other extraction systems. Thus, this work demonstrates that the same mechanism and energetics are operative for the formation of a third phase upon solvent extraction of mineral acids, independent of the chemical nature of the extractant.

Downloaded At: 08:40 25 January 2011

ACKNOWLEDGEMENTS

This work was supported by the U.S. Department of Energy, Office of Basic Energy Science, Division of Chemical Sciences, Biosciences and Geosciences under contract No. DE-AC02-06CH11357.

The submitted manuscript has been created by the University of Chicago as Operator of Argonne National Laboratory (“Argonne”) under Contract No. DE-AC02-06CH11357 with the U.S. Department of Energy. The U.S. Government retains for itself, and others acting on its behalf, a paid-up, nonexclusive, irrevocable worldwide license in said article to reproduce, prepare derivative works, distribute copies to the public, and perform publicly and display publicly, by or on behalf of the Government.

REFERENCES

1. Vasudeva Rao, P.R.; Kolarik, Z. (1996) A review of third phase formation in extraction of actinides by neutral organophosphorus extractants. *Solvent Extr. Ion Exch.*, 14: 955–993.
2. Erlinger, C.; Gazeau, D.; Zemb, Th.; Madic, C.; Lefrançois, L.; Hebrant, M.; Tondre, C. (1998) Effect of nitric acid extraction on phase behavior, microstructure and interactions between primary aggregates in the system dimethyldibutyltetradecylmalonamide (DMDBTDMA)/*n*-dodecane/water: A phase analysis and small-angle X-ray scattering (SAXS) characterisation study. *Solvent Extr. Ion Exch.*, 16: 707–738.
3. Erlinger, C.; Belloni, L.; Zemb, Th.; Madic, C. (1999) Attractive interactions between reverse aggregates and phase separation in concentrated malonamide extractant solutions. *Langmuir*, 15: 2290–2300.
4. Jensen, M.P.; Chiarizia, R.; Ferraro, J.R.; Borkowski, M.; Nash, K.L.; Thiyagarajan, P.; Littrell, K.C. (2002) New Insights in Third Phase Formation in the U(VI)-HNO_3, TBP-Alkane System. In *Proceedings of the International Solvent Extraction Conference ISEC 2002*, Sole, K.C.; Cole, P.M.; Preston, J.S.; Robinson, D.J., Eds.; South African Institute of Mining and Metallurgy, Marshalltown: 1137–1142.
5. Chiarizia, R.; Jensen, M.P.; Borkowski, M.; Ferraro, J.R.; Thiyagarajan, P.; Littrell, K.C. (2003) Third phase revisited: the U(VI), HNO_3/TBP, *n*-dodecane system. *Solvent Extr. Ion Exch.*, 21: 1–27.
6. Chiarizia, R.; Jensen, M.P.; Borkowski, M.; Ferraro, J.R.; Thiyagarajan, P.; Littrell, K.C. (2003) SANS study of third phase formation in the U(VI), HNO_3/TBP, *n*-dodecane system. *Sep. Sci. Technol.*, 38: 3313–3331.
7. Borkowski, M.; Chiarizia, R.; Jensen, M.P.; Ferraro, J.R.; Thiyagarajan, P.; Littrell, K.C. (2003) SANS study of third phase formation in the Th(IV), HNO_3/TBP, *n*-octane system. *Sep. Sci. Technol.*, 38: 3333–3351.
8. Chiarizia, R.; Nash, K.L.; Jensen, M.P.; Thiyagarajan, P.; Littrell, K.C. (2003) Application of the Baxter model for hard-spheres with surface adhesion to SANS data for the U(VI)-HNO_3, TBP-*n*-dodecane system. *Langmuir*, 19: 9592–9599.
9. Chiarizia, R.; Jensen, M.P.; Borkowski, M.; Thiyagarajan, P.; Littrell, K.C. (2004) Interpretation of third phase formation in the Th(IV)-HNO_3, TBP-*n*-octane system with Baxter’s “Sticky Spheres” model. *Solvent Extr. Ion Exch.*, 22: 1–27.
10. Nave, A.; Mandin, C.; Martinet, L.; Berthon, L.; Testard, F.; Madic, C.; Zemb, Th. (2004) Supramolecular organization of tri-*n*-butyl phosphate in organic diluent on approaching third phase transition. *Phys. Chem. Chem. Phys.*, 6: 799–808.
11. Chiarizia, R.; Jensen, M.P.; Rickert, P.G.; Kolarik, Z.; Borkowski, M.; Thiyagarajan, P. (2004) Extraction of zirconium nitrate by TBP in *n*-octane: Influence of cation type on third phase formation according to the “Sticky Spheres” model. *Langmuir*, 20: 10798–10808.
12. Plaue, J.; Gelis, A.; Czerwinski, K.; Thiyagarajan, P.; Chiarizia, R. (2006) Small angle neutron scattering study of plutonium third phase formation in 30% TBP/HNO_3/alkane diluent systems. *Solvent Extr. Ion Exch.*, 24: 283–298.
13. Chiarizia, R.; Rickert, P.G.; Stepinski, D.; Thiyagarajan, P.; Littrell, K.C. (2006) SANS Study of third phase formation in the HCl-TBP-*n*-octane system. *Solvent Extr. Ion Exch.*, 24: 125–148.
14. Chiarizia, R.; Stepinski, D.C.; Thiyagarajan, P. (2006) SANS study of third phase formation in the extraction of HCl by TBP isomers in *n*-octane. *Sep. Sci. Technol.*, 41: 2075–2095.
15. Chiarizia, R.; Briand, A. (2007) Third phase formation in the extraction of inorganic acids by TBP in *n*-octane. *Solvent Extr. Ion Exch.*, 25: 351–371.
16. Chiarizia, R.; Briand, A.; Jensen, M.P.; Thiyagarajan, P. (2008) SANS study of reverse micelles formed upon the extraction of inorganic acids by TBP in *n*-octane. *Solvent Extr. Ion Exch.*, 26: 333–359.
17. Zalupski, P.R.; Mc Alister, D.R.; Stepinski, D.C.; Herlinger, A.W. (2003) Metal extraction by silyl-substituted diphosphonic acids. III. Ester group substituent effects on phosphoryl oxygen basicity. *Solvent Extr. Ion Exch.*, 21: 331–345.
18. Tanford, C. (1972) Micelle shape and size. *J. Phys. Chem.*, 76: 3020–3024.
19. Thiyagarajan, P.; Urban, V.; Littrell, K.C.; Ku, C.; Wozniak, D.G.; Belch, H.; Vitt, R.; Toeller, J.; Leach, D.; Haumann, J.R.; Ostrowski, G.E.; Donley, L.I.; Hammonds, J.; Carpenter, J.M.; Crawford, R.K. (1998). *The performance of the Small-Angle Diffractometer SAND at IPNS, in ICANS XIV, The Fourteenth Meeting of the International Collaboration on Advanced Neutron Sources*, Starved Rock Lodge, Utica, IL, June 14–19, 1998, vol. 2: 864–878.
20. Pedersen, J.S. (1997) Analysis of small-angle scattering data from colloids and polymer solutions: Modeling and least-square fittings. *Adv. Colloid Interface Sci.*, 70: 171–210.
21. Baxter, R.J. (1968) Percus-Yevick equation for hard spheres with surface adhesion. *J. Chem. Phys.*, 49: 2770–2774.
22. Menon, S.V.G.; Kelkar, V.K.; Manohar, C. (1991) Application of Baxter’s model to the theory of cloud points of nonionic surfactant solutions. *Phys. Rev. A*, 43: 1130–1133.

23. Goyal, P.S.; Menon, S.V.G.; Dasannacharya, B.A.; Thiyagarajan, P. (1995) Small-angle neutron scattering study of micellar structure and interparticle interactions in triton X-100 solutions. *Phys. Rev. E*, 51: 2308–2315.
24. Antonio, M.R.; Chiarizia, R.; Gannaz, B.; Berthon, L.; Zorz, N.; Hill, C.; Cote, G. (2008) Aggregation in solvent extraction systems containing a malonamide, a dialkylphosphoric acid and their mixtures. *Sep. Sci. Technol.*, 43: 2572–2605.
25. Vandegrift, G.F. (1984) Diluents for TBP extraction systems. In: *Science and Technology of Tributyl Phosphate*. Schulz, W.W.; Navratil, J.D., Eds.; CRC Press: Boca Raton, FL, Vol. 1: 69–136.

Downloaded At: 08:40 25 January 2011